Multi-Modal Multi-Role UAV: Conceptual Study

Alexandru Daniel PREDA*

*Corresponding author
Doctoral School of Faculty of Aerospace Engineering,
National University of Science and Technology POLITEHNICA Bucharest,
Splaiul Independentei 313, 060042, Bucharest, Romania,
preda.alexdaniel@gmail.com

DOI: 10.13111/2066-8201.2025.17.3.6

Received: 11 August 2025/ Accepted: 25 August 2025/ Published: September 2025

Abstract: *This paper presents the conceptual design of a modular unmanned aerial vehicle (UAV) platform featuring vertical/conventional take-off and landing (VTOL/CTOL) and interchangeable cabin modules tailored for different mission profiles, aimed at enhancing operational flexibility and reducing logistical complexity, thereby improving overall economic efficiency. The study addresses aerodynamic, structural, and propulsion aspects of a unified UAV configuration that can be reconfigured for a variety of missions, including cargo and passenger transport, intelligence, surveillance and reconnaissance (ISR), medical evacuation (MEDEVAC/CASEVAC), search and rescue (SAR), combat/escort support, and electronic warfare (EW). A parametric analysis of propulsion sizing, aerodynamic performance, wing structural loading and landing gear sizing is conducted to assess the feasibility of the concept. The modular approach aims to enables significant cost savings, shorter turnaround times, and reduced logistical burden, without compromising mission capability.*

Key Words: *conceptual design, modular UAV, VTOL/CTOL capabilities, multi-mission, multi-engine, hybrid propulsion, wing ducted fan, reducing logistical complexity, improving economic efficiency*

1. INTRODUCTION

This paper introduces a new class of UAV: the modular one. It also explains how this aim could be achieved. Although there are currently aircraft dedicated to specific mission profiles (fixed wing, rotary wing and unmanned platforms), there is no single platform capable of performing all of these missions. In this article, a summary description of this new concept drone, which defines an entirely new class of UAVs, namely the **Multi-Modal Multi-Role U.A.V. (M.M.-M.R. U.A.V.)**, or short said **Modular UAV (M.U.A.V.)**, will be presented, based on the theoretical and engineering analysis developed within the current doctoral research underdevelopment of the article's author.

This article therefore aims to provide a technical overview of the new proposed concept.

2. MODULAR UAV – CONCEPTUAL STUDY

2.1 M.U.A.V. – Technical Specifications

- Max Take-Off Weight (MTOW) / Max Payload / Max. Fuel: 5000 / 1000 / 1000 kg;
- Wingspan: 22m;

- Operational Ceiling: FL400;
- Max Ceiling (for ISR missions): FL500;
- Cruising speed: 687 km/h @ FL400;
- Hybrid propulsion system for VTOL/HOVER: 1 turboshaft engine drives 2 electrical generators, which in turn supply power to 6 electric motors;
- 2 coaxial rotors with D = 3,7 m, H/D ratio = 0,057, each rotor disk being driven by a Safran GENeUS 300 electric motor (four such motors in total);
- 2 coaxial rotors with D = 2,5 m, H/D ratio = 0,057, each rotor disk being driven by a Siemens SP260 electric motor (two such motors in total);
- HOVER capability in OGE (Out of Ground Effect) up to a max. altitude of 1.840 m;
- Propulsion system for conventional forward flight: 2 x GE HF120 turbofan engines;
- Landing gear: tricycle-type, retractable;
- Empennage configuration: Twin-Boom / Twin-Tail layout, featuring 2 vertical stabilizers integrated with the twin booms, and 3 horizontal stabilizers (the conventional left/right horizontal stabilizers plus a 3rd horizontal surface linking the 2 vertical fins).

As defined and developed in the conceptual design study, the modular UAV consists of two main components:

1. The interchangeable mission module;
2. The fixed structure.

2.2 M.U.A.V. – Interchangeable Mission Module

Depending on the mission requirements, a dedicated ***mission module/cabin*** is mounted onto this fixed structure.

The reconfiguration is performed on the ground in a straightforward manner by sliding the mission module along two T-profile guide rails positioned on the upper side of the cabin and a third T-profile rail located on the lower side.

The 3D design and structural modeling were performed in Autodesk Fusion 360.

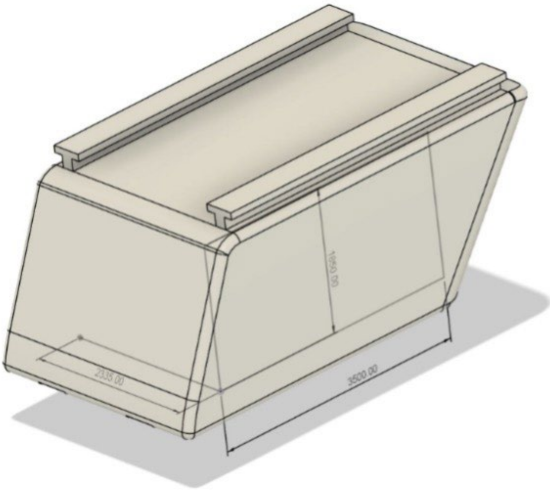

Figure 1. – Perspective view of the module/cabin

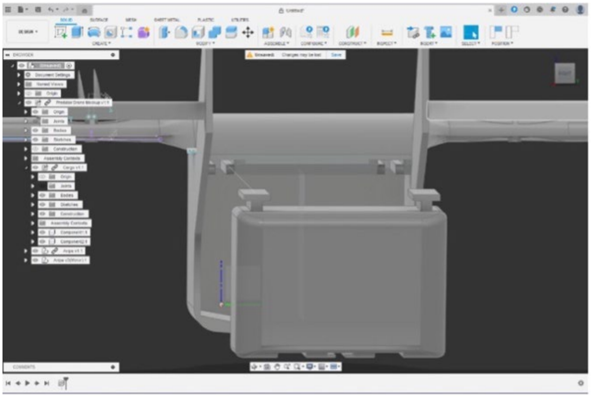

Figure 2. – Module – Fixed Structure Joint movement

Depending on the mission profile, the interchangeable module/cabin offers the following payload capabilities:

- Cargo: 1000 kg;
- Pax: 10 fully equipped personnel;
- Med/CasEVAC: 1 Intensive Care & Advanced Life Support / 4 dedicated stretcher positions plus 4 seated positions;
- Combat (used in Escort missions for Cargo/SAR/MedEvac or Combat Air Patrol): 12 missiles (2 x AIM-120 AMRAAM, 2 x AIM-132 ASRAAM, 2 x AGM-114 Hellfire, 2 x Brimstone, 2 x APKWS II and 2 x MBDA SeaVenom); layout: 2 launch racks designed similarly to a vertical parking structure (*see Figure 3*), so as a missile is ready for launch, the belly hatch of the fuselage opens for deployment.

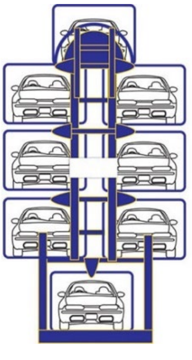

Figure 3. – Vertical Parking Structure

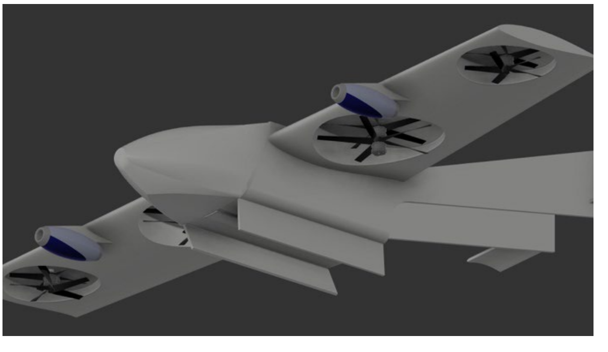

Figure 4. – Belly hatch in "Open" position

- SAR: 1 stretcher and 4 seated positions; the rescue hoist/winch is mounted inside the cabin, allowing access through the belly hatch (similar to Combat configuration). A full range of rescue devices can be employed including harnesses, suspension strops or stretcher/basket;
- ISR / EW: for these mission types, an analysis is required to determine whether the available space in the avionics bay is sufficient to accommodate the full suite of equipment. Some payloads, such as the EO/IR turret, will be externally mounted.

2.3 M.U.A.V. – Fixed Structure

The ***fixed structure*** comprises the primary airframe (fuselage, wings, empennage), the propulsion systems, the landing gear, the avionics suite, and the electrical power supply system.

2.3.1 M.U.A.V. Propulsion System

The ***propulsion system*** is designed to meet the specific requirements of the intended missions while complying with EASA provisions. In particular, the available thrust must be sized with a safety factor (FoS) of 10% [1].

Thus, for VTOL flights, in smooth vertical takeoff condition (acceleration 0,05 g / 0,5 m/s²) or hover flights, the following thrust requirement was determined:

$$T_{VTOL} = m\ x\ (g + a)\ x\ FoS\ =\ 5000kg\ x\ \left(9{,}80665\frac{m}{s^2} + 0{,}496\frac{m}{s^2}\right)\ x\ 1{,}1 = 56664\ N \quad (1)$$

The thrust distribution (*see Figure 5*) is configured at 70% to the large diameter rotors (3,7m) and 30% to the smaller rotors (2,5m).

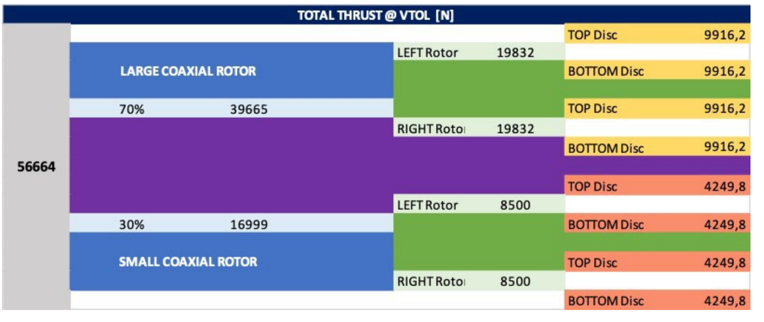

Figure 5. – Thrust distribution of Large / Small Rotor 70% - 30%

The system is also sized to remain operational under ***critical conditions***, specifically in the event of a failure of one large rotor disk during hover. In this scenario, the thrust that would have been generated by the failed disk is redistributed as follows: 60% to the remaining 3 large disks and 40% to the 4 smaller disks *(see Figure 6)*.

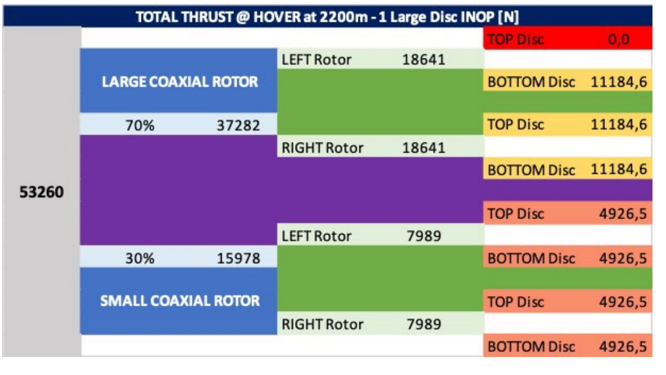

Figure 6. – Thrust Distribution in a Critic Scenario of 1 large rotor blade INOP

To ensure the required thrust for VTOL and hover, the propulsion architecture is configured as follows: 1 x Safran Makila 2A1 turboshaft engine drives 2 x Honeywell 1 MWh electric generators. These, through dedicated power electronics (inverters, converters, etc.), supply 3 electric motors each, which in turn drive the 4 coaxial rotor assemblies.

The overall efficiency of the system is calculated at 88,18% resulting from:

- Siemens SP260 electric motor efficiency (2 units) – 95%;
- Safran GENeUS300 electric motor efficiency (4 units) – 96%;

- Power electronics efficiency – 95%;
- Honeywell 1MW electric generator efficiency – 97%

$$\eta_{propulsion\ system} = \frac{(2*0{,}95)+(4*0{,}96)}{6} * 0{,}95 * 0{,}97 = 0{,}8818 = 88{,}18\% \tag{2}$$

The total weight of the propulsion system required for VTOL/Hover is 1143 kg, distributed as follows:

- Turboshaft engine: 279kg;
- Gearbox – Transferbox – Shafts: 100kg;
- Electric generators: 254kg;
- Power electronics: 156kg;
- Electric motors: 250kg;
- Wiring: 33kg;
- Propellers: 71kg.

In summary, the architecture of this system is as illustrated below:

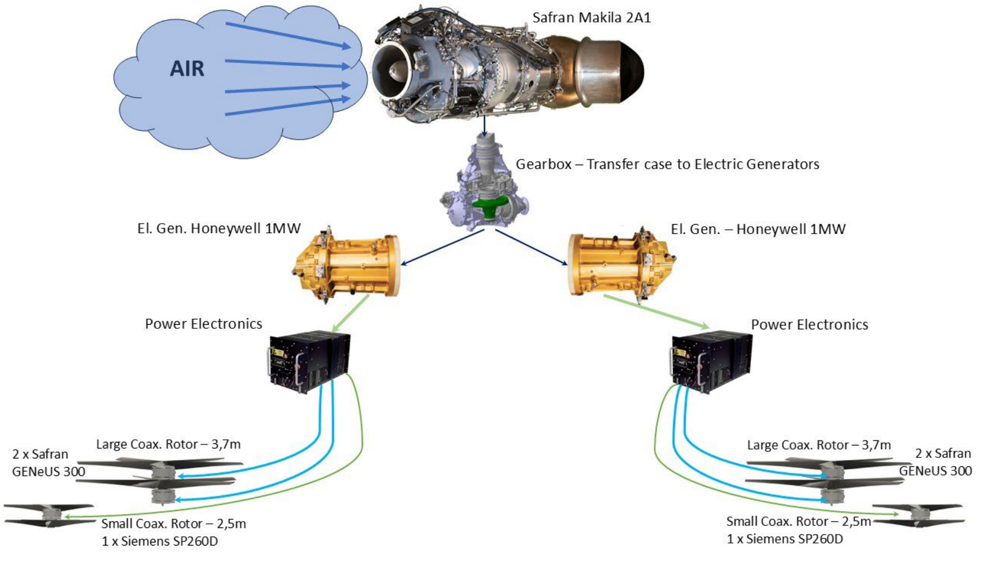

Figure 7. – Diagram of propulsion and transmission system for VTOL / HOVER capability

Regarding the climbing and cruising flight phases, which are powered by 2 turbofan engines, the governing formula is as follows:

$$T = D = \frac{1}{2}\rho V^2 S C_d + m * g * FoS * \sin\theta \tag{3}$$

Since the required thrust varies with altitude, the air density at each point of interest was computed for improved accuracy using the following equation:

$$\rho_{FL} = \frac{p_0 * \left(1 - \frac{L*h}{T_0}\right)^{\frac{g}{R*L}}}{R*(T_0 - L*h)} \tag{4}$$

Based on the calculation performed, and also considering the weight reduction due to fuel burn (TSFC = 71 Kg/kN/h), the necessary thrust was determined to be:

Table 1. – Thrust required during climbing flight depending on the FL, speed, air density, climbing angle

		kg/m3	RoC [m/s] TAS	V [m/s]	S [m2]	Cd	Total Thrust [kN]	Thrust/engine [kN]		climbing gradient	γ
	FL500	0,20395	3,33	190,80		0,004063782	2,2	1,1		0,0175	1,00
	FL400	0,31167	9,70	185,34		0,004267984	4,8	2,4		0,0523	3,00
	FL300	0,45831	12,00	172,03		0,011589600	10,6	5,3		0,0698	4,00
	FL250	0,54895	17,00	162,64		0,008596971	11,0	5,5		0,1045	6,00
	FL200	0,65270	22,00	158,08		0,010418920	14,9	7,4		0,1392	8,00
ρ	FL150	0,77082	25,00	143,97	88,83	0,010418920	16,6	8,3		0,1736	10,00
	FL100	0,90464	24,00	138,21		0,010958670	17,6	8,8		0,1736	10,00
	FL050	1,05555	18,00	129,34		0,012338110	17,1	8,6		0,1392	8,00
	Alt 500m	1,16728	15,00	123,08		0,011589600	15,6	7,8		0,1219	7,00
	FL010	1,18957	10,00	114,74		0,009942160	11,6	5,8		0,0872	5,00
	Alt 150m	1,20747	3,50	100,29		0,007174206	5,7	2,9		0,0349	2,00
	Alt 30m	1,22149	1,50	85,95		0,004157345	2,6	1,3		0,0175	1,00

Therefore, the 2 turbofan engines selected for climb and cruise are the same as those used on the HondaJet family, developed by Honda in partnership with General Electric: **GE HF120**, each providing a maximum thrust of 9,31 kN.

In conclusion, the total weight of the propulsion system is 1.565 kg.

Furthermore, based on the similar calculation the cruise flight range is determined:

Table 2. – MUAV's mass evolution during the cruise flight regarding the burned fuel

MUAV's mass evolution during the cruise flight											
Cruising Ceiling		Cruising Flight Time									
FL500		30 MIN	60 MIN	90 MIN	120 MIN	150 MIN	180 MIN	210 MIN	240 MIN	270 MIN	300 MIN
MUAV Mass [kg]	4810,7	4731,0	4651,8	4573,1	4495,0	4417,4	4340,3	4263,7	4187,6	4112,1	4037,0
Total Fuel Burned [kg]	189,3	79,7	79,2	78,7	78,1	77,6	77,1	76,6	76,1	75,6	75,1
Thrust [kN]		*2,25*	*2,23*	*2,22*	*2,20*	*2,19*	*2,17*	*2,16*	*2,14*	*2,13*	*2,11*
Remaining Fuel [kg]	810,7	730,9	651,7	573,1	494,9	417,3	340,2	263,7	187,6	112,0	37,0

We notice that after 270 min of cruising, there are 112 kg of fuel in the tanks. Further, we'll calculate if this is enough for the descend and landing phases:

$$T = D = \frac{1}{2}\rho V^2 S C_d - m * g * FoS * \sin\theta \tag{5}$$

Table 3. – Thrust required during descend flight depending on the FL, speed, air density, climbing angle

		kg/m3	RoD [m/s] TAS	V [m/s]	S [m2]	CD	Total Thrust [kN]	Thrust/engine [kN]	descent gradient	γ
	FL500	0,20395	16,51	189,42		0,004063782	-2,5	-1,3	0,0872	5,00
	FL400	0,31167	13,97	170,49		0,004267984	-1,9	-1,0	0,0819	4,70
	FL300	0,45831	11,94	152,15		0,011589600	2,0	1,0	0,0785	4,50
	FL250	0,54895	10,92	149,12		0,008596971	1,4	0,7	0,0732	4,20
	FL200	0,65270	9,65	145,63		0,010418920	3,5	1,8	0,0663	3,80
ρ	FL150	0,77082	8,38	137,29	88,83	0,010418920	4,1	2,0	0,0610	3,50
	FL100	0,90464	6,86	126,81		0,010958670	4,7	2,4	0,0541	3,10
	FL050	1,05555	5,59	114,39		0,012338110	5,5	2,7	0,0488	2,80
	Alt 500m	1,16728	4,06	97,04		0,011589600	3,9	1,9	0,0419	2,40
	FL010	1,18957	3,05	79,40		0,009942160	1,7	0,8	0,0384	2,20
	Alt 150m	1,20747	2,03	72,77		0,007174206	0,8	0,4	0,0279	1,60
	Alt 30m	1,22149	0,76	62,37		0,004157345	0,4	0,2	0,0122	0,70

Table 4. – Total mass of fuel burned during descent and landing

	Seconds	Fuel Burned [kg]
FL500 - FL400	184,6	-9,3
FL400 - FL300	218,2	-8,3
FL300 - FL250	127,7	5,0
FL250 - FL200	139,5	4,0
FL200 - FL150	157,9	10,9
FL150 - FL100	181,8	14,6
FL100 - FL050	222,2	20,8
FL050 - 500M	183,3	19,8
500m - FL010	47,4	3,6
FL010 - 150M	50,8	1,7
150M - 30M	59,1	1,0
30M - 0M	39,4	0,3
TOTAL =	1611,8	81,6

We can conclude that the total:

a) flight time is 5h 16' 16", composed by:

- Take-Off and Climbing – 19 min. 24 sec.;
- Cruising – 270 min.;
- Descent and Landing – 26 min. 52 sec.

b) range of flight is 3502,7 km, composed by:
   - Take-Off and Climbing – 186,3 km;
   - Cruising – 3091,5 km (4,5h*687km/h);
   - Descent and Landing – 224,9 km.

During this envelope, the total amount of fuel burned was 969,6 kg.

2.3.2 M.U.A.V. – Fixed/Rotary Wing Configuration

Regarding the fixed wing **architecture and geometry:**

- High wing layout: to allow unobstructed ground access around the aircraft and to maximize ground clearance for the turbofan engines;
- Wingspan: 22m;
- Mean chord 4,25;
- Wing area: 93,5m^2;
- Airfoil: NACA 64A318 (root) and NACA 64A412 (wingtip);
- Root chord length: 5m;
- Wingtip chord length: 3,5m;
- Taper ratio: 0,7;
- Wing loading: 53,47 kg/m2;
- Max. thickness: 18% @ 37,74% of the mean chord length;

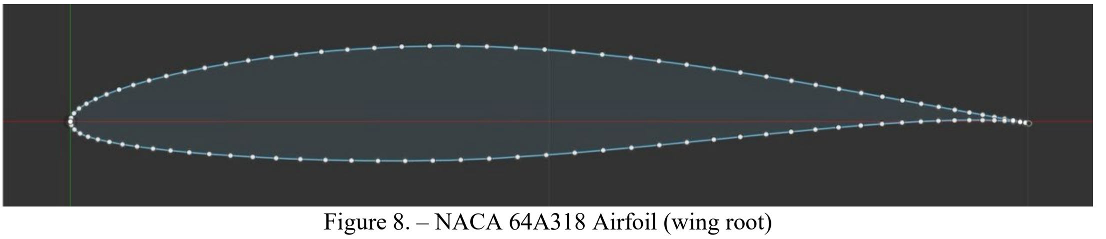

Figure 8. – NACA 64A318 Airfoil (wing root)

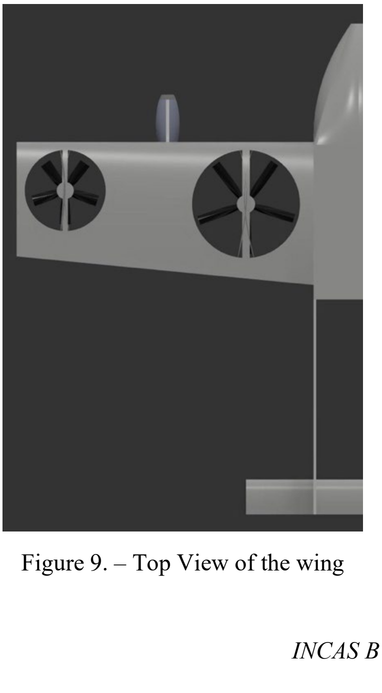

Figure 9. – Top View of the wing

As a particular feature, each wing's upper surface is equipped with 4 butterfly-style hatches. These are open when the embedded rotors are in use and close during climb or cruise phases, ensuring the airflow over the upper surface remains as laminar and undisturbed as possible.

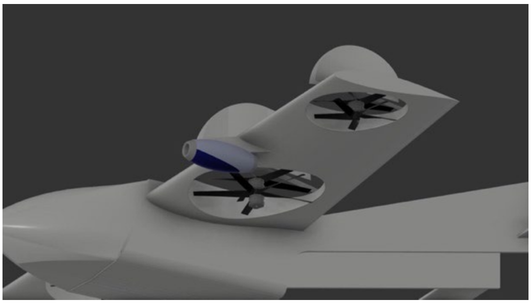

Figure 10. – Bottom side view of the wing

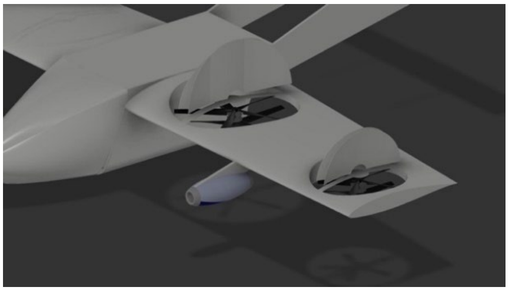

Figure 11. – Upper side view of the wing

From the wing structural analysis perspective, the maximum shear force and the maximum bending moment along the wing, considering main spar sized, load distribution, spanwise geometry while complying with EASA's provisions [2], are calculated.

Therefore:

- Max. shear force (at the wing root): V_x = 17920,7 N;

$$\boldsymbol{V_x = -\sum_{i=1}^{n} F_i * H(x - x_i) + \sum_{j} -w_j * [\left(x - x_{start_j}\right) * H\left(x - x_{start_j}\right) - (x - x_{final_j}) * H\left(x - x_{final_j}\right)] - \int_{x}^{11} q(x)dx} \tag{6}$$

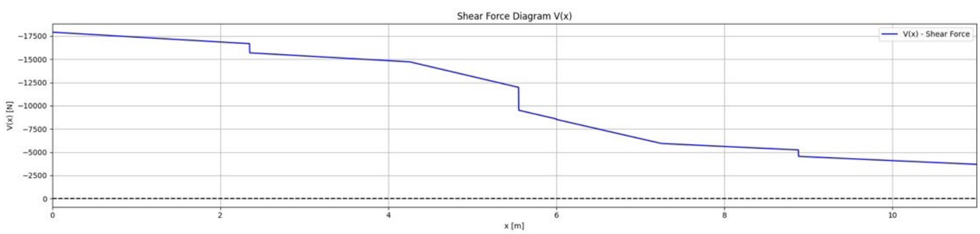

Figure 12. – Shear force distribution along the wing

- Max. bending moment (at the wing root): M_x = -117840,9 Nm

$$M_x = \sum[-\boldsymbol{F_i} * (\boldsymbol{x} - \boldsymbol{x_i}) * \boldsymbol{H}(\boldsymbol{x} - \boldsymbol{x_i})] - \sum \boldsymbol{w_j}\left[\frac{\left(\boldsymbol{x} - \boldsymbol{x_{start_j}}\right)^2}{2} * \boldsymbol{H}\left(\boldsymbol{x} - \boldsymbol{x_{start_j}}\right) - \frac{\left(\boldsymbol{x} - \boldsymbol{x_{final_j}}\right)^2}{2}\boldsymbol{H}\left(\boldsymbol{x} - \boldsymbol{x_{final_j}}\right)\right] - \int_0^x \boldsymbol{w_s} * (\boldsymbol{x} - \boldsymbol{s})\boldsymbol{ds} \tag{7}$$

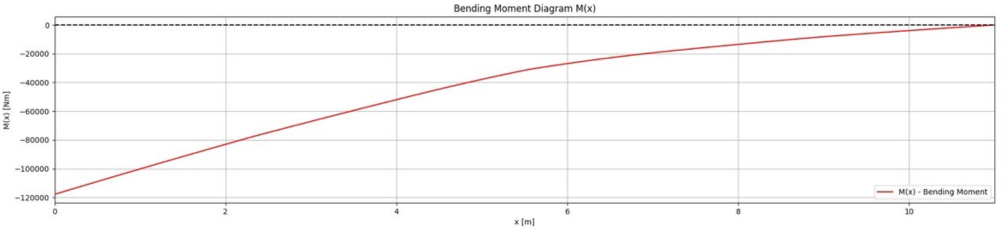

Figure 13. – Bending Moment along the wing

Regarding the *rotary-wing*, the blades of the coaxial rotors use a NACA 4412 airfoil. Furthermore, to enhance aerodynamic performance, each of the 5 blades of a disc incorporates a progressive twist across 5 sections.

Figure 14 – Coaxial rotor, twisted blade airfoil

By introducing a twist (θ_{twist}) along the blade span, the design ensures that each radial section operates at its local optimum angle of attack (α_{optim}) based on the relative airflow velocity at a given radial distance *r*. This optimum angle corresponds closely to the angle of maximum lift coefficient (17° – for the large rotor, 14° – for the small rotor) but is typically reduced by 1–2 degrees to maintain a safety margin and avoid stall.

In this configuration with two sets of coaxial rotors used, each with different diameters and therefore different Reynolds numbers (Re = 342677 for the large rotor and Re = 154275 for the small rotor), we'll have 2 values of optimum angle:

a) $\alpha_{optimLarge} = 15^0$ – for the large rotor – Diameter = 3.7m;

b) $\alpha_{optimSmall} = 12^0$ – for the small rotor – Diameter = 2.5m;

The blade twist distribution is governed by the following equations [3]:

$$\theta_{twist} = \theta_{flux} - \alpha_{optim} \tag{8}$$

$$\theta_{flux} = \text{atan}\left(\frac{v_{induced}}{v_{tang(r)}}\right) \tag{9}$$

	r	ω_{rotor}	Vtang	Vinduced	θ_{flux}	α optim	θ_{twist}	Vrelative
R=1.85m	0,3		6,06		72,64		57,64	20,33
	0,6875		13,89		54,39		39,39	23,86
	1,075	20,21	21,73	19,4	41,76	15	26,76	29,13
	1,4625		29,56		33,28		18,28	35,36
	1,85		37,39		27,42		12,42	42,12
R=1.25m	0,2		3,96		78,11		66,11	19,21
	0,4625		9,15		64,04		52,04	20,91
	0,725	19,79	14,35	18,8	52,65	12	40,65	23,65
	0,9875		19,54		43,89		31,89	27,12
	1,25		24,74		37,23		25,23	31,07

Figure 15. – Blade Twist Distribution

As a result of this twist distribution, the following aerodynamic improvements were calculated:

- decreasing drag by 37,4% in the case of the large-diameter rotor and by 7,7% for the small-diameter rotor);
- improved aerodynamic finesse: +19,9% for the large rotor and +11,1% for the smaller rotor.

2.3.3 M.U.A.V. – Landing Gear Configuration

The **Landing gear** – taking into consideration all the mission profiles which the Modular UAV should cover, the aerodynamics advantages and ground handling easiness, a retractable landing gear is chosen instead of a simple skid configuration. The retractable configuration is tricycle with the main landing gear having 2 struts left/right and the nose landing gear – 1 strut.

In the proposed configuration, the main landing gear is designed to absorb approximately 85% of the total impact energy, with the remaining 15% being dissipated through the nose landing gear. Unlike the static load, which is primarily determined by the aircraft's weight during ground operations, the dynamic load during landing impact involves significantly higher transient forces due to vertical descent velocity and energy transfer through the landing gear structure. For this dynamic load, a factor of safety (FoS) of 2 has been adopted, exceeding the EASA-mandated minimum of 1.5, in order to ensure structural integrity and operational reliability under the harsh environmental and mission conditions anticipated for the MUAV.

In order to correctly dimension the main landing gear and nose landing gear, several key components must be accurately calculated to achieve a robust, lightweight, and reliable landing gear system suitable for multi-role operational demands. These include:

a) tire's Maximum Bottoming Load (MBL): it represents the maximum load that the tire could absorb without to bring any harm to the tire's internal structure;

$$\frac{MBL}{MTOW} = 1{,}951$$

b) static and dynamic loads;

Static:	Dynamic:
Main landing gear: $\frac{0{,}85*m*g}{2}$	Main landing gear: $\frac{0{,}85*m*g*FoS}{2}$
Nose landing gear: $0{,}15*m*g$	Nose landing gear: $0{,}15*m*g*FoS$

c) the impact energy absorbed during landing (which dictates the required damping capacity);

$$E_{impact} = \frac{mV_{vert}{}^2}{2}, \tag{10}$$

v_{vert} = vertical component of the speed during the landing = 3m/s (600fpm) [4]

$$E_{impact} = E_{tyre} + E_{shockabsorber}, \#(10) \tag{11}$$

$$F_{shockabsorber}(x) = kx \tag{12}$$

$F_{tyre} \leq$ MBL

δ_{tyre} = maximum tyre deflection

d) the maximum shock absorber force (which determines structural resistance under peak loads. Also, we'll consider that the force will act linearly;

$$E_{shockabsorber} = \int_0^s F_{shockabsorber}(x)dx, \tag{13}$$

$$E_{tyre} = F_{tyre} * \delta_{tyre}, \tag{14}$$

e) strut geometry (essential for ensuring proper energy dissipation and mechanical strength), including:
   - stroke length = s = 0,15m;
   - piston diameter (considering $P_{piston}max = 2*10^7$Pa & $P_{piston}extended = 8*10^6$Pa):

$$F_{piston}max = P_{piston}max * A_{piston} \tag{15}$$

$$F_{piston}max = P_{piston}max * \frac{\pi D_{piston}max^2}{4} => D_{piston}max = \sqrt{\frac{4 * F_{piston}max}{\pi * P_{piston}max}} \tag{16}$$

   - strut diameter: ~ 20-22mm larger than the piston diameter;

f) nitrogen pre-charge and compression pressures, as well as the gas volume variations, must be optimized to provide sufficient cushioning without bottoming-out or over pressurization during high-energy impacts:

$$P_0 * V_0 = P_1 * V_1 => V_0 = V_1 * \frac{P_1}{P_0}, \tag{17}$$

P_0, V_0 = Initial nitrogen Pressure and Volume, when the shock absorber is fully extended;
P_1, V_1 = Final nitrogen Pressure and Volume, when the shock absorber is fully compressed;

$$V_0 = \Delta V * \frac{P_1}{P_1 - P_0}, \tag{18}$$

$$\Delta V = A_{piston} * s \tag{19}$$

$$A_{piston} = \frac{\pi {D_{piston}}^2}{4} \tag{20}$$

Therefore, the landing gear has the following characteristics:

Main Landing Gear (2 struts):		*Nose Landing Gear (1 strut):*
- Tire's MBL = 48,04 kN;		- Tire's MBL = 9,78 kN;
- Static load = 20839,1 N;		- Static load = 7345,9 N;
- Dynamic load = 41678,2 N		- Dynamic load =14871,9 N;
- Energy absorbed E_{impact} = 9562,5 J;		- Energy absorbed E_{impact} = 3375 J;
- Max. shock absorber force = 95,45 kN;		- Max. shock absorber force = 38,47 kN;
- Strut length = 550 mm;		- Strut length = 593 mm*;
- Stroke = 150 mm;		- Stroke = 150mm;
- Nitrogen pre-charge pressure: 80 bar;		- Nitrogen pre-charge pressure: 80 bar;
- Pressure at max. compression: 200 bar;		- Pressure at max. compression: 200 bar;
- Piston diameter: 77,96 mm;		- Piston diameter: 49,49 mm;
- Strut diameter: ~100mm;		- Strut diameter: ~70mm;
- Nitrogen Volume (extended): 1,19 L;		- Nitrogen Volume (extended): 0,48 L;
- Nitrogen Vol. (compressed): 0,47 L;		- Nitrogen Vol. (compressed): 0,19 L

** The 43 mm height difference accounts for the maximum tire diameter difference between the main and nose gear, ensuring that the aircraft waterline remains parallel to the ground.*

3. CONCLUSIONS

This paper has presented briefly the conceptual design and preliminary technical assessment of a Multi-Modal Multi-Role UAV (MM-MR UAV/MUAV) which is capable of fulfilling a wide variety of mission profiles using a single fixed airframe and interchangeable mission modules. The proposed architecture integrates a hybrid VTOL (turboshaft/electric) / CTOL (turbofan) propulsion system, high-wing layout with embedded coaxial rotors, and a modular payload cabin system, enabling rapid ground reconfiguration between operational roles such as cargo transport, ISR, SAR, MEDEVAC, and combat/escort support.

Aerodynamic analysis validated the wing geometry configuration, airfoil combination, and coaxial rotor blade twist distribution, with quantified improvements in lift-to-drag ratio and drag reduction for both large and small rotor sets. The design supports a maximum range of **3,500+ km** and a total flight endurance of over **5 hours** with the specified fuel load.

Structural analysis of the wing, based on shear force and bending moment distributions, confirmed compliance with relevant EASA provisions and demonstrated that the primary load-bearing members are adequately sized for the expected mission envelope.

The landing gear sizing was conducted for both static and dynamic load cases, incorporating energy absorption requirements, shock absorber stroke, piston geometry, nitrogen pre-charge parameters, and Maximum Bottoming Load (MBL) verification. The final configuration provides adequate safety margins above EASA minimum requirements for operation in demanding environments.

Overall, the results indicate that the MUAV configuration is technically feasible and capable of meeting the diverse mission requirements identified in the study.

Future work will focus on a finite element analysis (FEA) of the joint between the mission module's T-profile guide rails, and the fixed structure. This analysis will ensure structural integrity and prevent any deformation under flight loads and maneuvering conditions. A comprehensive flight stability analysis will also be conducted, particularly in hover conditions, to ensure the aircraft meets handling quality requirements.

In addition, dedicated studies will address the transition phase from VTOL to forward flight. These studies will look at the aerodynamic and control aspects involved in gradually reducing the thrust generated by the embedded electric rotors while increasing the thrust provided by the turbofan engines. The aim is to achieve a smooth and stable transition between flight regimes.

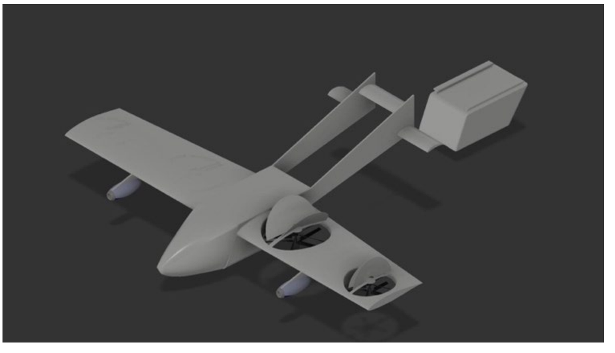

Figure 16. – Upper side view of the Modular UAV

In the end of this chapter, is worth mentioning that in this configuration, this design has been accepted and published in the Community Designs Bulletin of the EUIPO, holding Registration Certificate No. 015097502-0001, which stands as a confirmation of the innovative element brought to this field.

REFERENCES

[1] * * * European Aviation Safety Agency. *AMC Nr. 1 – CS 25.101(c)*, January 2023. Available at https://www.easa.europa.eu

[2] * * * European Aviation Safety Agency. *CS-29, Amendment 12 / 26.11.2024, CS-29.303.* Available at https://www.easa.europa.eu

[3] J. G. Leishman, *Principles of Helicopter Aerodynamics*, 2nd edition, Cambridge University Press, ISBN: 978-1-107-01335-3, page 129.

[4] * * * https://skybrary.aero/articles/hard-landing